Surfactant-free fabrication of pNIPAAm microgels in microfluidic devices

Mutian Hua, Yingjie Du, Jiaqi Song, Mo Sun, and Ximin He[a)]
Department of Materials Science and Engineering, University of California Los Angeles, Los Angeles, California 90024, USA

(Received 1 June 2018; accepted 4 September 2018)

Conventional pNIPAAm microgel synthesis utilizes surfactants to suspend pre-gel droplets in the immiscible continuous phase due to the slow polymerization required for synthesizing pNIPAAm in aqueous solvent. To improve the fabrication process and to eliminate the effects of surfactant on microgel quality, a surfactant-free and water-free method was developed. Rapid polymerization of high-quality microgels was achieved in a single-channel microfluidic device to help maintain the integrity of gel particles without the addition of surfactants. The droplet generation mechanism and the effect of flow rate of the two in-going immiscible fluid on the geometry of the produced microgels were studied. The produced microgels have low polydispersity with a dispersity index of 6.4%. The pNIPAAm hydrogels fabricated in the DMSO solvent has smaller pore size and more uniform microstructure compared to that synthesized in water. The fabricated pNIPAAm microgels show a sharp volume phase transition at ~32 °C and high deswelling/swelling rate.

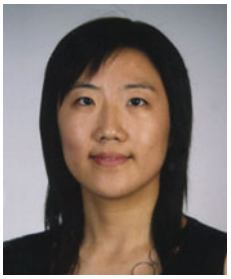

Ximin He

Ximin He is an assistant professor of Materials Science and Engineering at University of California, Los Angeles, and Faculty of California Nanosystems Institute (CNSI). Dr. He was postdoctoral research fellow in Wyss Institute of Bioinspired Engineering and School of Engineering and Applied Science with Professor Joanna Aizenberg at Harvard University. Dr. He received her Ph.D. in Chemistry in the fields of Nanoscience and Organic Optoelectronics from University of Cambridge, Melville Laboratory for Polymer Synthesis, Cavendish Laboratory and Nanoscience Center. Dr. He's research focuses on biologically inspired functional smart materials, chemical and biological sensors, actuators with broad applications in materials science, biomedicine, environment, and energy. Dr. He is the recipient of the NSF CAREER award, AFOSR Young Investigator Program award, Harvard Postdoctoral Award for Professional Development, Gates Cambridge Scholarship, U.K. Overseas Research Scholarship, the Government Award for National Outstanding Students, and U.K. National Excellent Young Scientist Award.

I. INTRODUCTION

Responsive microgels are crosslinked micron/submicron sized polymeric particles that can swell or deswell in response to external stimuli.[1] The osmosis nature of hydrogels' volume changing mechanism makes microgels extremely advantageous in achieving fast (de)swelling rate due to their reduced diffusion distance and increased surface area compared to bulk gels. Due to their unique thermal responsive behaviors, poly(*N*-isopropylacrylamide) (pNIPAAm) microgels hold exceptional interest in broad research areas such as environmental, biomedical, and energy fields. pNIPAAm hydrogels can undergo a reversible volume phase transition at its lower critical solution temperature (LCST) around 32 °C.[2,3] Compared with other types of stimuli responsive hydrogels such as pH responsive gels, the sharp transition of pNIPAAm from hydrophilic to hydrophobic phase is beneficial for achieving precise control and switching of the gel volume.[4] The thermal responsive property of pNIPAAm hydrogels also allows for remote and localized control of deformation by incorporating photo-absorbers that convert photonic energy into local heat in the material and is not easily achieved with other types of stimuli responsive hydrogels.[5,6] These unique properties of pNIPAAm microgels has attracted great attention in its applications in drug delivery,[7–13] sensing,[6,14–17] separation,[18] and purification.[19]

In biomedical fields, hydrogels are commonly used as cell culturing scaffolds and have received increasing attention in applications such as tissue-engineered organoids (organ mimics).[20–22] Hydrogels have similar elastic modulus to tissues and are biocompatible, which facilitate

[a)]Address all correspondence to this author.
e-mail: ximinhe@ucla.edu
DOI: 10.1557/jmr.2018.364

cell attachment and growth. The porous microstructure also allows for nutrient and waste diffusion in or out of the gel, which is essential for cell viability. The engineered tissue models are highly advantageous in gaining insight into disease pathophysiology and identifying new therapies.[20] Large microgels with diameter on the order of tens or hundreds of microns can be especially useful in tissue engineering for their close resemblance to the geometry of vascular, bone marrow, or alveoli-like tissues.[20,23–25] Fabricating pNIPAAm large microgels with diameter of few hundred microns could provide new possibilities in organ mimics.

Conventional synthesis methods such as emulsion polymerization and precipitation polymerization can produce gel particles on the order of nanometer or submicrometer with low poly-dispersity.[26,27] Fabricating pNIPAAm microgels with diameter on the order of tens or hundreds of microns by emulsion synthesis can be challenging due to the inability to well suspend larger droplets of pre-gel solution in the continuous phase. The templating method was developed to overcome this obstacle, where sacrificial mesoporous templates of desired size was used to hold pre-gel solution during emulsion polymerization.[28] The templating polymerization method requires first trapping the pre-gel solution within the template particles and then remove the template after polymerization, which is associated with higher cost and extra steps. More advanced methods using microfluidic devices can produce large microgels on the order of tens or hundreds of microns in a single step, where droplets of pre-gel solution are generated in series inside a continuous phase followed by the polymerization of monomers in these droplets.[29–32] The microfluidic devices often require a capillary orifice that allows the continuous phase to hydrodynamically focus the pre-gel solution to create droplets. The glass capillaries are often drawn by hand and therefore is difficult to reproducibly fabricate more than one at a time. Microfluidic devices constructed using soft-lithography or direct molding of silicon elastomer poly(dimethylsiloxane) (PDMS) are more parallel in production and thus can be replicated in large quantities.

Water is often used as a solvent for microfluidic synthesis of pNIPAAm microgels due to the immiscibility of the monomer *N*-isopropylacrylamide (NIPAAm) aqueous solution with wide selections of organic solvents.[26,31,33,34] Aqueous droplets containing the monomers generated inside the microfluidic device are crosslinked using thermally activated initiator ammonia persulfate (APS). Additional infusion of an accelerator *N*, *N*,*N*′,*N*′-tetramethylethylenediamine (TEMED) is needed after droplet generation to initiate the polymerization under room temperature. The water-based synthesis of pNIPAAm microgels requires multiple inlets and is associated with more complex channel structures. As NIPAAm becomes less miscible in water at elevated temperature near or above 32°, the polymerization must be controlled to take place slowly to avoid precipitation of pNIPAAm from the aqueous phase induced by polymerization heat. To prevent merging between droplets prior to full polymerization, surfactants are often added as the particle stabilizer. However, the presence of surfactants has been reported to interfere with the polymerization process, increase the LCST of produced microgels, and affect cell viability.[35–38] Therefore, laborious sequential washing and centrifuge steps have been used to purify and sediment the gel particles. A surfactant-free method to produce microgels is needed to overcome the dilemma between the simplification of fabrication and the microgel quality.

Here we present a surfactant-free method for fabricating pNIPAAm microgels based on water-free rapid polymerization of pNIPAAm microgels in PDMS microfluidic device. The produced microgels are easily collected and purified due to the surfactant-free attributes. The microfluidic device is also simplified with only one straight channel due to the single-step infusion of all reactants. Detailed characterization of the synthesized pNIPAAm hydrogels were conducted to investigate the influence of solvent and flow rate on their microstructure, geometry, and thermal properties.

II. EXPERIMENTAL

A. Materials

N-isopropylacrylamide (NIPAAm, 98%) was purchased from Acros Organics and purified via recrystallization from hexane prior to use to remove the inhibitor. *N*, *N*′-methylenebisacrylamide (BIS, Sigma-Aldrich, St. Louis, Missouri), 2-hydroxy-2-methylpropiophenone (Daracure1173, TCI America, Portland, Oregon), ammonia persulfate (APS, Acros Organics, Somerville, New Jersey), dimethyl sulfoxide (DMSO, Fisher Chemical, Fair Lawn, New Jersey), *n*-octane (98%, Acros Organics, Somerville, New Jersey), SYLGARD 184 silicone elastomer kit (Krayden, Midland, Michigan), PE tubing (ID 0.015″, OD 0.043″, BD Intramedic), and double side adhesive sheet (Artgrafix, Beacon Falls, Connecticut) were used as purchased.

B. Fabrication of microfluidic device

The microfluidic channel pattern was cut in a 300 μm thick double-sided adhesive sheet using a laser cutter. The channel has a dimension of 14 mm (L) × 800 μm (W) × 300 μm (H) with two inlet holes and one outlet hole. PDMS sealing was fabricated by mixing SYLGARD 184 elastomer base and catalyst with a 10:1 ratio, the mixture was degassed and molded into 3 mm thick PDMS sheet. Inlet and outlet holes on the PDMS sealing were punctured using a biopsy with 0.8 mm diameter

before device assembly. The sandwich microfluidic device was fabricated by placing the laser-cut double-sided adhesive sheet on a glass substrate followed by stacking PDMS sealing on top of the double-sided adhesive [Fig. 1(a)]. All three components were oxygen plasma treated for 2 min before assembly to improve adhesion between layers.

C. Synthesis of microgels

The pre-gel solution containing 20 wt% NIPAAm, 1 wt% BIS, and 1 wt% Daracure1173 in DMSO and the continuous phase *n*-octane were separately injected into the assembled microfluidic channel using syringe pumps (Harvard Apparatus Ph.D. Ultra & Harvard Apparatus 55-1111). These two immiscible fluids form a biphasic laminar flow through the microfluidic channel and at the location of outlet, the pre-gel solution forms droplets in the continuous *n*-octane phase, as discussed in detail in Sec. III. The flow rates of the two inlets were controlled separately to allow for precisely controlling and tuning the size and geometry of the produced pre-gel droplets. The pre-gel droplets were carried downstream through the outlet tubing and passed under a 40 W UV fiber lamp. Thus, the monomers in the pre-gel droplets photopolymerized and were UV-crosslinked to form solid hydrogel droplets. The produced microgels were sedimented by gravity in an ethanol bath for collection. The control sample of pNIPAAm microgel synthesized in water was fabricated following the same procedure as described above with pre-gel solution containing 20 wt% NIPAAm, 1 wt% Bis, and 1 wt% Daracure 1173 in DI water.

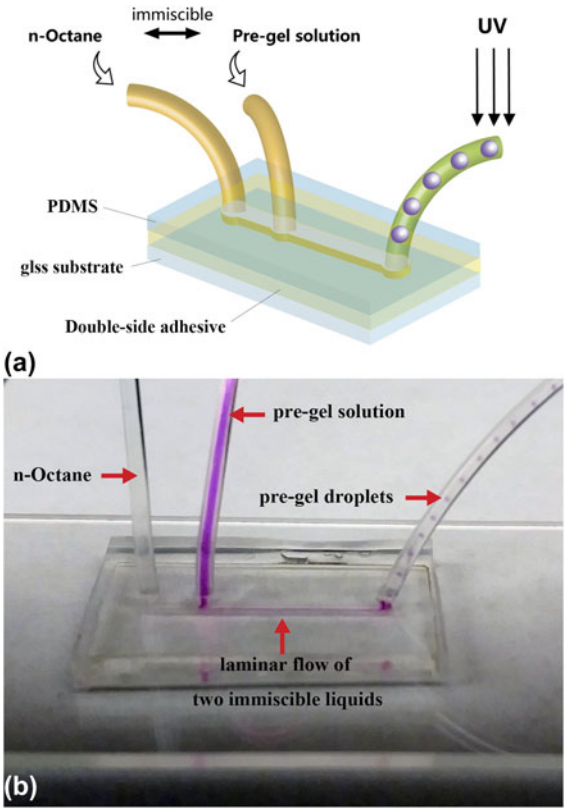

FIG. 1. (a) Schematic of the microfluidic device and (b) laminar flow and droplet generation inside the microfluidic device. The pre-gel solution is dyed with Rhodamine B for visual observation.

D. Microgel purification

The supernatant was removed from the ethanol bath to remove *n*-octane, DMSO, and unreacted monomers dissolved in ethanol. The microgels were then placed inside a 50 °C oven overnight to completely evaporate the residual *n*-octane, DMSO, and ethanol. The dried microgel samples were rehydrated with water for further characterization.

E. Synthesis of pNIPAAm hydrogels in water and DMSO

Bulk pNIPAAm hydrogels were synthesized in water and DMSO to study the solvent effect on hydrogel microstructures. 20% NIPAAm + 1% Bis + 1% APS in water and 20% NIPAAm + 1% Bis + 1% Daracure 1173 in DMSO were used as the pre-gel solution. 500 μL of pre-gel solutions were pipetted into a 2 mL glass vial, respectively. For polymerizing pNIPAAm hydrogel in water solvent, 10 μL of TEMED was injected into the vial followed by vortexing for 2 s. The gelation process finished in around 10 s. For polymerizing pNIPAAm hydrogel in DMSO, the glass vial containing pre-gel solution was exposed under a 40 W UV fiber lamp for 10 s to obtain a crosslinked gel.

F. Characterization of pNIPAAm hydrogels

The pNIPAAm hydrogels synthesized using water/DMSO as the solvent were immersed in deionized water for 48 h to remove unreacted monomers. The hydrogels were cut open to expose internal structures and freeze-dried to preserve the 3D structure of the polymer networks. The dried samples were mounted onto scanning electron microscopy stubs using conductive tape and imaged using ZEISS Supra 40VP SEM (Carl Zeiss AG, Toronto, Canada).

The morphology of pNIPAAm microgels was imaged using a Leica DMI 6000B (Leica Microsystems, Buffalo Grove, Illinois) optical microscope. Microgel solution was put inside a petri dish for characterization using transmission bright field mode of the microscope. The focal plane was carefully adjusted to show the largest cross-sectional area of the microgels.

G. Measurement of swelling ratio

The microgels synthesized using water/DMSO as the solvent were immersed in deionized water inside a petri dish for at least 48 h to reach equilibrium prior to measurement. A PID controlled heater and a temperature sensor were fixed inside the petri dish. The water

temperature can be accurately maintained at the set temperature through automated on/off switching of the heater. The microgel size was recorded using an optical microscope at different bath temperatures. The volume of the microgel was calculated by assuming a spherical geometry. The swelling ratio by volume was calculated using the following formula:

$$\text{Swelling ratio (SR)} = \frac{V}{V_0} \quad ,$$

where V_0 is the equilibrium volume under room temperature and V is the volume recorded under different temperatures. For LCST measurement, the bath temperature was kept at each point for 20 min to allow the gel to reach its equilibrium volume.

For deswelling/swelling rate measurement, the pNIPAAm microgels were restricted to a small area inside the empty petri dish by spacer prior to measurement. Water with ~50 °C temperature was poured into the petri dish to initiate deswelling. The cross-sectional size of the microgels was captured using the optical microscope with 2-s frame intervals. The swelling ratios of the microgels were calculated using the above equation. The reswelling rate for the pNIPAAm microgels were measured by first extracting the hot water in the petri dish and refill immediately with ice water. Recording process and volume conversion were same as above.

III. RESULT AND DISCUSSION

A. Pre-gel droplet formation

In conventional synthesis of microgels, surfactants are used as the particle stabilizer to prevent merging between colliding pre-gel droplets. To eliminate the use of surfactants, rapid polymerization of the pre-gel droplets must be achieved. Thus, the pre-gel droplets are fully polymerized before collision could happen, ensuring the integrity of each particle. However, rapid polymerization may not be desirable when water is used as the solvent due to the insolubility of pNIPAAm at elevated temperature. In this study, we have used DMSO as the solvent for polymerizing pNIPAAm microgels because pNIPAAm does not exhibit the volume phase transition in DMSO. Rapid polymerization of pNIPAAm microgels could be achieved by the water-free synthesis.

pNIPAAm microgels were fabricated in the microfluidic device by using DMSO as the pre-gel solution solvent. An immiscible liquid *n*-octane was used as the continuous phase. Photo-initiator and UV flooding were used to realize the rapid polymerization chemistry. Due to the one-step infusion of all reactants, the microfluidic device is simplified to single channel, in comparison to conventional designs where multiple channels are needed for step-wise infusion of reactants. The device simplification also benefits from the water-free chemistry. The pre-gel droplet formation mechanism is discussed below.

The Reynolds number is an important dimensionless quantity that predicts the flow pattern of liquids inside microfluidic channels. For a channel with a rectangular cross section, the Reynolds number can be calculated using the following formula:

$$\text{Re} = \frac{4Q\rho}{P\mu} \quad ,$$

where Q is the volumetric flow rate of liquid, ρ is the density of liquid, P is the wetted perimeter, and μ is the dynamic viscosity of the liquid.

The pre-gel solution using DMSO as the solvent has a Reynolds number between 0.11 and 0.63 when the flow rate changes from 2 to 20 μL/min, while the continuous phase has the corresponding Reynolds number between 1.84 and 2.35. The low Reynolds number of the flowing liquids suggests the formation of laminar flow inside the microfluidic channel. This was confirmed by adding Rhodamine B as a fluorescent dye into the pre-gel solution for visual observation of the droplet generation process (Rhodamine B was not included in the actual microgel synthesis and was used here for imaging purposes only). Side-by-side biphasic laminar flow of the pre-gel solution and the continuous phase was formed inside the channel between the two immiscible liquids [Fig. 1(b)]. The biphasic laminar flow was maintained along the full length of the microfluidic channel. The interface for both liquids decreased significantly as the biphasic laminar flow entered the narrower outlet tubing. The laminar flow became less stable with decreasing wetted perimeter. The pre-gel stream was hydrodynamically focused by the continuous phase stream at the narrower outlet and broke into monodisperse droplets as the two liquids enter the outlet tubing. The formed pre-gel droplets are carried downstream by the continuous phase and photo-polymerized before collision could occur between the pre-gel droplets.

B. Size and geometry control

pNIPAAM microgels with well-controlled different sizes and geometries were successfully produced by varying the pre-gel solution (DMSO solvent) flow rate from 2 to 20 μL/min, while the continuous phase flow rate was kept at 50 μL/min. Higher flow rates were attempted but tended to lead to failure at the PDMS-double side adhesive bonded interface due to high internal pressure. The morphologies of microgels synthesized in DMSO solvent produced at different pre-gel solution flow rates are shown in Fig. 2. The produced microgels were spherical when the pre-gel solution flow rate was not higher than 3.5 μL/min [Figs. 2(a) and 2(b)],

with lower pre-gel solution flow rates producing smaller particle sizes. This result is consistent with the higher local shear created at the outlet between the two phases at higher continuous phase to pre-gel solution flow rate ratio. The microgels' shape changed from spherical to ellipsoidal then to capsule shape with the increasing flow rate of the pre-gel solution [Figs. 2(c)–2(e)]. This resulted from the outlet tubing size restriction where larger droplets were forced to elongate along the tubing direction. The axis perpendicular to the tubing was maintained at ~400 μm for the microgels produced at pre-gel solution flow rate higher than 3.5 μL/min. Nonuniform beads composed of mixtures of microspheres, microcapsules, and long rods were produced when the flow rate for pre-gel solution exceeded 15 μL/min [Fig. 2(f)]. With more pre-gel solution flowing through the channel, a larger number of pre-gel droplets were generated in higher density and therefore had higher probability to merge with each other before being fully polymerized. The capability of easily manipulating the microgels' geometry by simply tuning the flow rates and ratios has potential in fabricating microgels with complex structures for broad applications.

The produced microgels showed low polydispersity. The size distribution histogram of the spherical microgels synthesized at a pre-gel solution flow rate of 2 μL/min is shown in Fig. 3. Two hundred microgel particles were randomly chosen and their diameters were measured using ImageJ. The microgels have a mean particle diameter of 304 μm and a standard deviation of 19 μm. The dispersity index was as low as 6.4%, in comparison to the relatively higher particle size variation of 10% by using other methods [Ref. 31], which proves that this simple structured microfluidic device is capable of stably producing uniform microgels with low polydispersity.

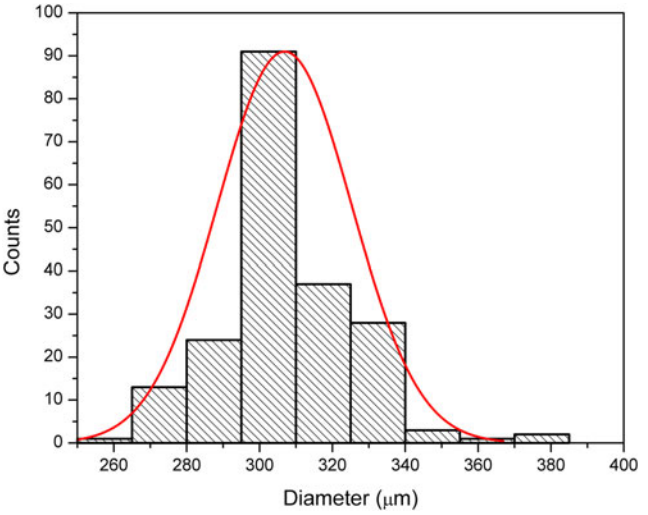

FIG. 3. Size distribution of the microgels fabricated using a pre-gel solution flow rate of 2 μL/min.

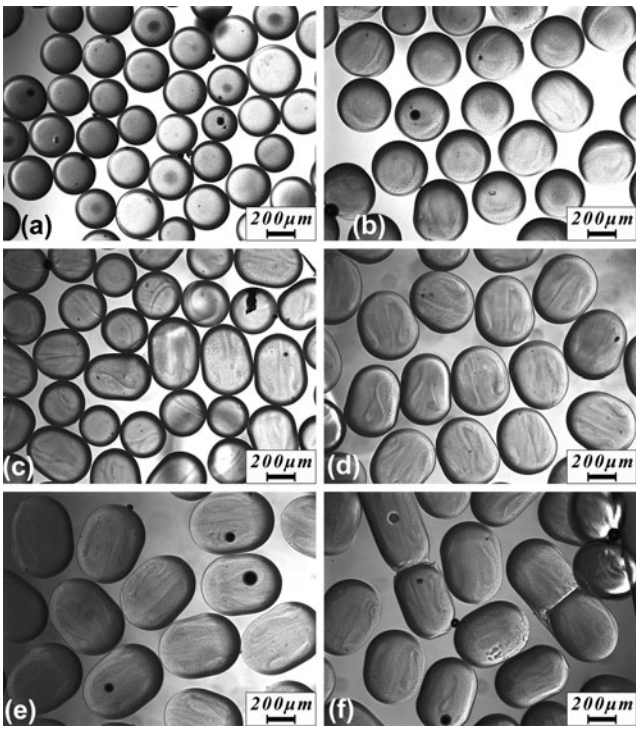

FIG. 2. Optical image of microgels fabricate using pre-gel solution flow rate from 2 μL/min (a) to 20 μL/min (f). The flow rate for *n*-octane was fixed at 50 μL/min.

C. Solvent effect on the microstructure of pNIPAAm hydrogels

Since pNIPAAm undergoes unique volume phase transition around 32 °C in aqueous environment, localized polymerization heat may lead to the insolubility or even precipitation of NIPAAm monomers out of the aqueous phase during the polymerization of pNIPAAm hydrogel. Figure 4 compares the color and the microstructures of pNIPAAm hydrogels synthesized using water [Fig. 4(a)] and DMSO [Fig. 4(b)] as a solvent. The amount of initiator was tuned so that both samples polymerized within the same short period of 10 s pNIPAAm hydrogels polymerized in water turned to white color, while hydrogels polymerized in DMSO

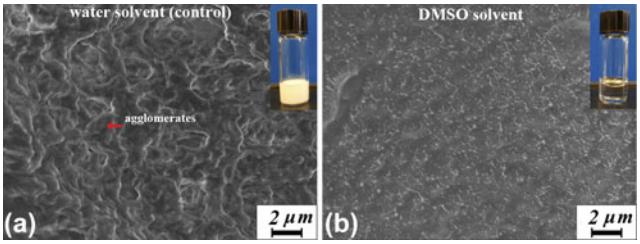

FIG. 4. Microstructure of pNIPAAm hydrogel synthesized in water (a) and DMSO (b). The inset shows the macroscopic color of the synthesized hydrogels.

stayed transparent. The white gel was incapable of becoming transparent again in water even after immersing in water for over 24 h. The permanent white color of the pNIPAAm hydrogels synthesized in water suggests that the formed polymer network has a microstructure that is incapable of dissolving in water, as verified by the SEM images [Fig. 4(a)].

Microscopic analysis under SEM shows that the pNIPAAm hydrogels synthesized in water has agglomerated polymer network with pore size around 1–5 μm. By contrast, pNIPAAm hydrogels synthesized in DMSO show more uniform microstructure with submicron pores. The agglomerates in pNIPAAm hydrogels synthesized in water may result from the hydrophobic aggregation of pNIPAAm networks when the polymerization heat is generated fast enough to raise the sample temperature above the LCST of pNIPAAm. The formed agglomerates were difficult to dissolve in water, which corresponds to the macroscopically unrecoverable white gel. Therefore, synthesizing pNIPAAm hydrogels in water tends to produce agglomerated polymers that has minimum interaction with water, which may lead to low thermosensitivity, reduced swelling ratio, and a more gradual volume phase transition. Using organic solvents such as DMSO to replace water is more advantageous because it not only accommodates rapid polymerization that allows for a surfactant-free synthesis of pNIPAAm hydrogels but also maintained or even enhanced hydrogel quality.

D. Thermally responsive behaviors of rapidly polymerized pNIPAAm microgels

The swelling ratios of the pNIPAAm microgels synthesized in water and DMSO have been studied as shown in Fig. 5. The insets in Fig. 5 are the corresponding optical image of microgels under 26 and 38 °C. Here, we use the microgels fabricated under a pre-gel solution flow rate of 2 μL/min because the spherical microgel deforms isotopically in all directions and the particle volume can be accurately converted from the cross-sectional area captured under the optical microscope. The microgels produced in DMSO show a large volume reduction of 64% when temperature increased from 25 to 38 °C. By contrast, the microgels produced in water have much smaller volume reduction of only 28%, which confirms that with an aggregated polymer network, the swelling ratio of pNIPAAm microgels synthesized in water significantly decreased, which defeats the intrinsic thermoresponsive functions of pNIPAAm. Additionally, 90% of the total volume reduction took place between 30 and 33 °C for the microgels produced in DMSO. The LCST of microgels produced in DMSO is the mid-point 31.5 °C, which is in accordance with the known volume phase transition temperature around 32 °C for pNIPAAm. The LCST of the produced microgels was not affected by using DMSO as a solvent and the rapid synthesis. By contrast, the 90% volume reduction temperature range expanded to between 28 and 33 °C for the microgels produced in water. This result suggests that the known sharp volume phase transition behavior becomes more gradual when pNIPAAm is rapidly polymerized in water.

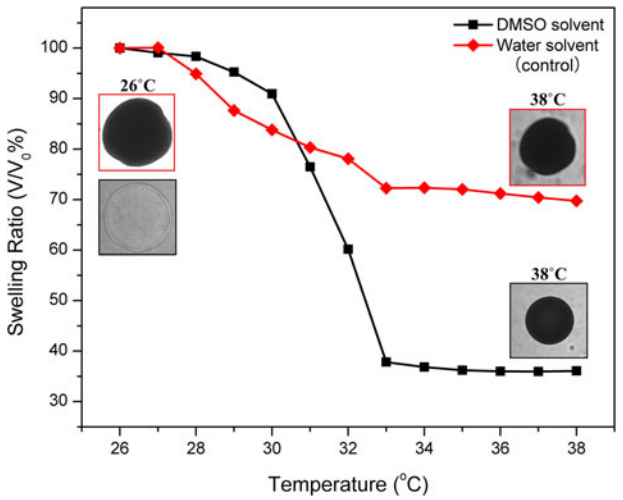

FIG. 5. Swelling ratio versus temperature curve of the microgels fabricated using a pre-gel solution flow rate of 2 μL/min.

The response rate of the pNIPAAm microgels were characterized by plotting the swelling ratio versus time curve. Figure 6(a) shows the deswelling rate of the microgels. The volume of microgels reduced exponentially after immersing in 50 °C water for 70 s. The microgels produced in DMSO shows steeper slope in comparison with the microgels produced in water. For achieving the same degree of shrinking from to 80% of the original volume, microgels produced in DMSO used 8 s while microgels produced in water used 65 s. More than 8 times faster deswelling rate was achieved. The reswelling rate of the same particle is shown in Fig. 6(b), faster swelling rate of the microgels produced in DMSO was also observed in comparison to relatively slower reswelling, and hysteresis observed in the microgels produced in water. This further indicates the high quality and good performance of the microgels produced by our method. The total volume reduction captured during the 70-s rapid deswelling was smaller than the volume reduction at the equilibrium value. This could be explained by the continuously reduced pore size during shrinking, which slowed down the water diffusion out of the gel. The reswelling rates were 8–10 times slower than deswelling and the microgel particles recovered to their original volume after 200 s. The slower reswell process was in accordance with the trend seen in most osmosis gels. Overall, the pNIPAAm microgels synthesized in DMSO well maintained the desirable thermal response rate, which was comparable to the standard swelling/deswelling kinetics of pNIPAAm.[39,40] The exhibited fast

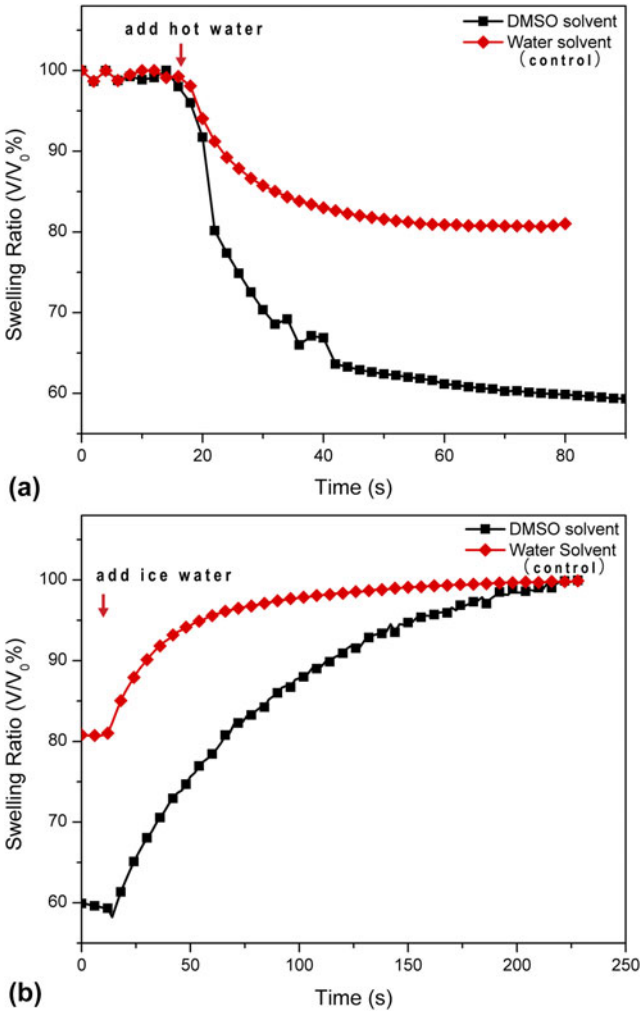

FIG. 6. Deswelling (a) and swelling (b) kinetics of pNIPAAm microgels fabricated using a pre-gel solution flow rate of 2 μL/min.

thermal responsiveness and large volume change ratio of our pNIPAAm microgels successfully eliminated the compromised thermal volume changing issue associated with the conventionally fabrication methods.

IV. CONCLUSION

In this work, we presented a surfactant-free method for synthesizing pNIPAAm microgels with low polydispersity based on water-free rapid polymerization. This innovative method has allowed for device simplification and optimized experimental procedures without sacrificing the microgel quality. Easy manipulation of microgel size and geometry was achieved by tuning the flow rate of the pre-gel solution. Microgels produced with our proposed method showed low dispersity index ~6.4% and exhibited sharp volume phase transition behavior as well as ~8 times faster response rates in comparison with microgels produced in water solvent. The proposed fabrication method could have broad application in sensing, separation, and biomedical research studies that involve production of large quantities of microgels with good thermal responsiveness. The chemistry and analysis presented could also provide insight on emulsion fabrication and fluid dynamics.

REFERENCES

1. B.R. Saunders and B. Vincent: Microgel particles as model colloids: Theory, properties and applications. *Adv. Colloid Interface Sci.* **80**, 1 (1999).
2. M. Heskins and J.E. Guillet: Solution properties of poly(*N*-isopropylacrylamide). *J. Macromol. Sci. Part A—Chem.* **2**, 1441 (1968).
3. H.G. Schild and D.A. Tirrell: Microcalorimetric detection of lower critical solution temperatures in aqueous polymer solutions. *J. Phys. Chem.* **94**, 4352 (1990).
4. R. Pelton: Temperature-sensitive aqueous microgels. *Adv. Colloid Interface Sci.* **85**, 1 (2000).
5. A. Sutton, T. Shirman, J.V.I. Timonen, G.T. England, P. Kim, M. Kolle, T. Ferrante, L.D. Zarzar, E. Strong, and J. Aizenberg: Photothermally triggered actuation of hybrid materials as a new platform for in vitro cell manipulation. *Nat. Commun.* **8**, 14700 (2017).
6. A.C. Manikas, A. Aliberti, F. Causa, E. Battista, and P.A. Netti: Thermoresponsive PNIPAAm hydrogel scaffolds with encapsulated AuNPs show high analyte-trapping ability and tailored plasmonic properties for high sensing efficiency. *J. Mater. Chem. B* **3**, 53 (2015).
7. B.S. Pattni, V.V. Chupin, and V.P. Torchilin: New developments in liposomal drug delivery. *Chem. Rev.* **115**, 10938 (2015).
8. N. Murthy, Y.X. Thng, S. Schuck, M.C. Xu, and J.M.J. Fréchet: A novel strategy for encapsulation and release of proteins: Hydrogels and microgels with acid-labile acetal cross-linkers. *J. Am. Chem. Soc.* **124**, 12398 (2002).
9. T.R. Hoare and D.S. Kohane: Hydrogels in drug delivery: Progress and challenges. *Polymer* **49**, 1993 (2008).
10. S.H. Choi, J.J. Yoon, and T.G. Park: Galactosylated poly(*N*-isopropylacrylamide) hydrogel submicrometer particles for specific cellular uptake within hepatocytes. *J. Colloid Interface Sci.* **251**, 57 (2002).
11. G-H. Hsiue, S. Hsu, C-C. Yang, S-H. Lee, and I-K. Yang: Preparation of controlled release ophthalmic drops, for glaucoma therapy using thermosensitive poly-*N*-isopropylacrylamide. *Biomaterials* **23**, 457 (2002).
12. T-M. Don, K-Y. Lu, L-J. Lin, C-H. Hsu, J-Y. Wu, and F-L. Mi: Temperature/pH/Enzyme triple-responsive cationic protein/PAA-b-PNIPAAm nanogels for controlled anticancer drug and photosensitizer delivery against multidrug resistant breast cancer cells. *Mol. Pharm.* **14**, 4648 (2017).
13. J. Huang, M. Li, P. Zhang, P. Zhang, and L. Ding: Temperature controlling fiber optic glucose sensor based on hydrogel-immobilized GOD complex. *Sens. Actuators, B* **237**, 24 (2016).
14. P. Tseng, B. Napier, L. Garbarini, D.L. Kaplan, F.G. Omenetto: Functional, RF-trilayer sensors for tooth-mounted, wireless monitoring of the oral cavity and food consumption. *Adv. Mater.* **30**, 1703257 (2018).
15. S. Maji, B. Cesur, Z. Zhang, B.G. De Geest, and R. Hoogenboom: Poly(*N*-isopropylacrylamide) coated gold nanoparticles as colourimetric temperature and salt sensors. *Polym. Chem.* **7**, 1705 (2016).
16. Y. Liu, T. Shen, L. Hu, H. Gong, C. Chen, X. Chen, and C. Cai: Development of a thermosensitive molecularly imprinted polymer resonance light scattering sensor for rapid and highly selective

detection of hepatitis a virus in vitro. *Sens. Actuators, B* **253**, 1188 (2017).
17. Z. Guo, H. Sautereau, and D.E. Kranbuehl: Structural evolution and heterogeneities studied by frequency-dependent dielectric sensing in a styrene/dimethacrylate network. *Macromolecules* **38**, 7992 (2005).
18. X. He, M. Aizenberg, O. Kuksenok, L.D. Zarzar, A. Shastri, A.C. Balazs, and J. Aizenberg: Synthetic homeostatic materials with chemo-mechano-chemical self-regulation. *Nature* **487**, 214 (2012).
19. W. Yuanzi, C. Zhen, W. Shuigen, X. Wenli, and M. Shanyun: Protein purification by chemo-selective precipitation using thermoresponsive polymers. *Biopolymers* **109**, e23222 (2018).
20. D.C. Wilkinson, J.A. Alva-Ornelas, J.M.S. Sucre, P. Vijayaraj, A. Durra, W. Richardson, S.J. Jonas, M.K. Paul, S. Karumbayaram, B. Dunn, B.N. Gomperts: Development of a three-dimensional bioengineering technology to generate lung tissue for personalized disease modeling. *Stem Cells Transl. Med.* **6**, 622 (2016).
21. D.E. Backman, B.L. LeSavage, S.B. Shah, J.Y. Wong: A robust method to generate mechanically anisotropic vascular smooth muscle cell sheets for vascular tissue engineering. *Macromol. Biosci.* **17**, 1600434 (2017).
22. B.L. Ekerdt, C.M. Fuentes, Y. Lei, M.M. Adil, A. Ramasubramanian, R.A. Segalman, D.V. Schaffer: Thermoreversible hyaluronic acid-PNIPAAm hydrogel systems for 3D stem cell culture. *Adv. Healthcare Mater.* **7**, 1800225 (2018).
23. E. Mohagheghian, J. Luo, J. Chen, G. Chaudhary, J. Chen, J. Sun, R.H. Ewoldt, and N. Wang: Quantifying compressive forces between living cell layers and within tissues using elastic round microgels. *Nat. Commun.* **9**, 1878 (2018).
24. C. Shimbori, J. Gauldie, and M. Kolb: Extracellular matrix microenvironment contributes actively to pulmonary fibrosis. *Curr. Opin. Pulm. Med.* **19** 446–452 (2013).
25. A. Joshi, S. Nandi, D. Chester, A.C. Brown, and M. Muller: Study of poly(*N*-isopropylacrylamide-*co*-acrylic acid) (pNIPAM) microgel particle induced deformations of tissue-mimicking phantom by ultrasound stimulation. *Langmuir* **34**, 1457 (2018).
26. R.K. Shah, J-W. Kim, J.J. Agresti, D.A. Weitz, and L-Y. Chu: Fabrication of monodisperse thermosensitive microgels and gel capsules in microfluidic devices. *Soft Matter* **4**, 2303 (2008).
27. P.J. Dowding, B. Vincent, and E. Williams: Preparation and swelling properties of poly(NIPAM) "minigel" particles prepared by inverse suspension polymerization. *J. Colloid Interface Sci.* **221**, 268 (2000).
28. M. Kumoda, Y. Takeoka, and M. Watanabe: Template synthesis of poly(*N*-isopropylacrylamide) minigels using interconnecting macroporous polystyrene. *Langmuir* **19**, 525 (2003).
29. W.J. Duncanson, T. Lin, A.R. Abate, S. Seiffert, R.K. Shah, and D.A. Weitz: Microfluidic synthesis of advanced microparticles for encapsulation and controlled release. *Lab Chip* **12**, 2135 (2012).
30. H. Zhang, E. Tumarkin, R. Peerani, Z. Nie, R.M.A. Sullan, G.C. Walker, and E. Kumacheva: Microfluidic production of biopolymer microcapsules with controlled morphology. *J. Am. Chem. Soc.* **128**, 12205 (2006).
31. D. Sivakumaran, E. Mueller, and T. Hoare: Microfluidic production of degradable thermoresponsive poly(*N*-isopropylacrylamide)-based microgels. *Soft Matter* **13**, 9060 (2017).
32. W.H. Tan and S. Takeuchi: Monodisperse alginate hydrogel microbeads for cell encapsulation. *Adv. Mater.* **19**, 2696 (2007).
33. M. Annaka, T. Matsuura, M. Kasai, T. Nakahira, Y. Hara, and T. Okano: Preparation of comb-type *N*-isopropylacrylamide hydrogel beads and their application for size-selective separation media. *Biomacromolecules* **4**, 395 (2003).
34. R. Acciaro, T. Gilanyi, and I. Varga: Preparation of monodisperse poly(*N*-isopropylacrylamide) microgel particles with homogenous cross-link density distribution. *Langmuir* **27**, 7917 (2011).
35. W. Chi and Z. Shuiqin: Effects of surfactants on the phase transition of poly(*N*-isopropylacrylamide) in water. *J. Polym. Sci., Part B: Polym. Phys.* **34**, 1597 (2018).
36. A. Mirja and M.S. Liisa: Structural studies of poly(*N*-isopropylacrylamide) microgels: Effect of SDS surfactant concentration in the microgel synthesis. *J. Polym. Sci., Part B: Polym. Phys.* **44**, 3305 (2006).
37. L-T. Lee and B. Cabane: Effects of surfactants on thermally collapsed poly(*N*-isopropylacrylamide) macromolecules. *Macromolecules* **30**, 6559 (1997).
38. M.A. Partearroyo, H. Ostolaza, F.M. Goñi, and E. Barberá-Guillem: Surfactant-induced cell toxicity and cell lysis: A study using B16 melanoma cells. *Biochem. Pharmacol.* **40**, 1323 (1990).
39. T. Gan, Y. Guan, and Y. Zhang: Thermogelable PNIPAM microgel dispersion as 3D cell scaffold: Effect of syneresis. *J. Mater. Chem.* **20**, 5937 (2010).
40. S. Xing, Y. Guan, and Y. Zhang: Kinetics of glucose-induced swelling of P(NIPAM-AAPBA) microgels. *Macromolecules* **44**, 4479 (2011).